Thermophoresis in colloidal suspensions

2008 J. Phys.: Condens. Matter 20 153102

(http://iopscience.iop.org/0953-8984/20/15/153102)

IOP Publishing Journal of Physics: Condensed Matter

J. Phys.: Condens. Matter **20** (2008) 153102 (18pp) doi:10.1088/0953-8984/20/15/153102

TOPICAL REVIEW

Thermophoresis in colloidal suspensions

R Piazza[1] **and A Parola**[2]

[1] Dipartimento di Chimica, Materiali e Ingegneria Chimica, Politecnico di Milano, 20133 Milano, Italy
[2] Dipartimento di Fisica e Matematica, Università dell'Insubria, 22100 Como, Italy

E-mail: roberto.piazza@polimi.it and alberto.parola@mi.infm.it

Received 19 December 2007, in final form 21 February 2008
Published 25 March 2008
Online at stacks.iop.org/JPhysCM/20/153102

Abstract
Thermophoresis is particle motion induced by thermal gradients. Akin to other driven transport processes, such as the Soret effect in simple fluid mixtures, or electrophoresis and diffusiophoresis in colloidal suspensions, it is, both experimentally and theoretically, a challenging subject. Rather than being a comprehensive recollection, this review aims to be a critical re-examination of the experimental and theoretical tools used to investigate thermophoresis, and of some recent relevant results that may unravel novel aspects of colloid solvation forces. The perspectives of thermophoresis as a tool for particle manipulation in microfluidics are also emphasized.

Contents

1. Introduction

The investigation of the equilibrium properties of colloidal dispersions has yielded valuable and often unforeseen insights on statistical mechanics and condensed matter physics. Since the effective interaction potential between colloidal particles can be tuned by varying the solvent properties, colloids can indeed be prepared as model systems, displaying the same structural properties of an assemblage of 'big atoms' interacting via simple, well defined forces [1]. In other words, the collective ('colligative') properties of a colloidal suspension are largely insensitive to the specific physicochemical nature of the constituting particles. Further information can be gained by applying external body forces such as gravity, which render the suspension spatially inhomogeneous and allow us to extract fine details of colloidal phase behavior [2]. More generally, studies of disperse systems driven by external fields or under non-equilibrium conditions may unravel novel and interesting aspects of condensed matter behavior.

Yet, even simple non-equilibrium phenomena may conceal delicate problems, and pose serious theoretical challenges, dwelling in the very roots of statistical physics. Colloidal thermophoresis, the effect we shall deal with in this review, is probably a kind of 'archetypal' non-equilibrium problem. The question is the following: how is particle motion influenced by the presence of a uniform thermal gradient ∇T? The

experimental evidence is that, on top of random Brownian diffusion, the particles perform a steady drift towards the hot or the cold side. This is quite similar to what happens when an external driving force, such as gravity or an electric field, is applied to the suspension. However, no *real* external field is actually present. Since the kinetic energy associated with the drift motion is generally a tiny fraction of $k_B T$, one may try and adopt a strategy akin to linear response analysis of thermal transport coefficients to derive an 'effective' field yielding the same effects as ∇T on particle motion. Yet, this is far from being trivial: rather, as we shall see, theoretical routes are often strewn by booby traps. Provided that fallacious tracks are carefully avoided, the real challenge is however explaining the most striking experimental feature of thermophoresis, namely its peculiar sensitivity to the investigated system. Indeed, the amplitude of thermophoretic effect is not fixed by particle general bulk or surface physical properties, such as its size, material density, thermal conductivity, or total surface charge: rather, it seems to be subtly related to the detailed microscopic nature of the particle/solvent interface. Because of this, thermophoresis is much harder to understand than other field-driven transport effects such as electrophoresis. On the other hand, such a strong system specificity makes thermophoretic studies particularly promising for obtaining novel information on particle/solvent interactions.

Rather than an extensive and 'neutral' compilation of recent results, this review aims to be a critical analysis of the experimental and theoretical tools used to investigate thermophoresis in liquids, and of some selected findings that we regard as particularly relevant. Fully aware that this selection may be partly biased, we nonetheless hope that our choice may spur further experimental and theoretical investigations of this intriguing effect.

1.1. Some basic definitions

As we mentioned, thermophoresis is an additional particle transport mechanism brought in, on top of Brownian diffusion, by the presence of a thermal gradient. We shall then write the total mass flux as

$$J = -D\nabla c - cD_T\nabla T, \tag{1}$$

where D is the usual Brownian diffusion coefficient. For historical reasons, related to the study of thermal diffusion in simple liquid mixtures, D_T is generally called the 'thermal diffusion coefficient'[3]. Dimensionally, however, D_T is not a diffusion coefficient and, noticing that the steady-state thermophoretic velocity acquired by the particle is simply given by $v_T = -D_T\nabla T$, should rather be dubbed *thermophoretic mobility*, in analogy with other transport effects such as electrophoresis. Observing that the 'thermodynamic force' associated with a thermal gradient is actually $\nabla T/T = \nabla \ln T$, a more meaningful definition can be given by writing

$$J' = -D\frac{\nabla c}{c} - \tilde{D}_T\frac{\nabla T}{T}, \tag{2}$$

where J' is the mass flux per unit concentration and $\tilde{D}_T = TD_T$ is a *true* diffusion coefficient, which can profitably be compared with D.

Assuming a uniform thermal gradient directed along z, vanishing of the net mass flow leads to a steady-state concentration profile[4]

$$\frac{dc}{dz} = -cS_T\frac{dT}{dz}, \tag{3}$$

where $S_T = D_T/D = -1/c(dc/dT)$ is called, by analogy to thermal diffusion in liquid mixtures (see below), the *Soret coefficient*. With this definition, $S_T > 0$ when the particles move to the cold, displaying what we shall call a 'thermophobic' behavior. The coefficient S_T introduces a characteristic length scale

$$\ell_T = (S_T\nabla T)^{-1} = \frac{D}{v_T}, \tag{4}$$

that can be envisaged as that length scale over which thermophoretic drift eventually becomes dominant with respect to Brownian diffusion. A length scale with the same physical meaning can obviously be defined for colloidal motion driven by a true external field. For instance, in colloid settling under gravity, this role is played by the sedimentation length $\ell_g = D/v_S$, where v_S is the Stokes sedimentation velocity. However in this case ℓ_g is also simply related to the applied field as $\ell_g = k_B T/mg$, where m is the particle buoyant mass, while no similar identification is easily conceivable for ℓ_T. Notice finally that, even when $\nabla T = \text{const}$, the concentration profile is exponential, $c(z) = c_0 \exp(-z/\ell_T)$, only provided that S_T does not appreciably depend on T and c.

2. Related effects

Before embarking on the analysis of colloid thermophoresis, it is instructive to take a glance at closely related transport effects induced by thermal gradients in liquid mixtures or in dilute gases, which stand at the roots of the problem we are considering, and concur in providing the conceptual framework for particle thermophoresis in liquids. As we shall see, the comprehension of the basic mechanisms underlying thermophoresis in liquids may indeed benefit from what is known about thermal diffusion in liquid mixtures and particle thermophoresis in gases.

2.1. Thermal diffusion in liquid mixtures and solutions (Ludwig–Soret effect)

Thermal diffusion, or the Ludwig–Soret effect, is the 'molecular counterpart' of particle thermophoresis, and

[3] Equation (1) assumes that, as is often the case, the particle concentration c is small. For very concentrated suspensions, it is more appropriate using dimensionless concentration units, such as weight fractions w, and redefine the mass flux as $J_w = -D\nabla w - w(1-w)D_T\nabla T$, which is symmetrical in particle and solvent composition.

[4] Of course, in the presence of gravity, care should be taken to avoid the onset of convective effects, leading in general to a very different stationary state. We shall extensively deal with spurious convection effects in what follows.

consists in the partial segregation of the components in fluid mixtures or simple solutions induced by a thermal gradient [3]. Originally discovered by Ludwig [4] by observing that concentrated salt solutions easily crystallize around the cooled limb of an inverted U-tube, it was later independently described by Soret [5], who quantified the effect for many electrolyte solutions, and clearly framed into non-equilibrium thermodynamics by de Groot [6]. Even though it is a relatively small effect (the Soret coefficient of common mixtures is only of the order of 10^{-3} K^{-1}), thermal diffusion has been extensively studied due to its dramatic impact on convective mixing. Indeed, since any inverted concentration gradient brought in by the Soret effect can relax only by mass diffusion, which is far slower than heat diffusivity, the convection threshold in mixtures is dramatically lowered compared to simple fluids (when $S_T < 0$, it is even possible to induce convection by heating from *above* [7]). Therefore, thermal diffusion plays a crucial role in many naturally occurring convective processes, from component segregation in solidifying metallic alloys [8] and volcanic lava [9] to convection in the earth mantle [10]. As already evident from the original observations by Ludwig, it also plays an important role in crystal growth [11]. More recently, it has been shown that thermal diffusion sets the scene for giant fluctuations in non-isothermal mixtures [12].

No detailed microscopic model of the Soret effect has so far been proposed. However, for gas mixtures, some general indications stem from kinetic theory. Thermal diffusion was indeed theoretically *predicted* by Chapman back in 1912 [13]. Chapman's explicit formulas are too complicated to be quoted here, so we shall recall only the main features of his results. First of all, thermal diffusion exists only if the masses $m_{1,2}$ or sizes $\sigma_{1,2}$ of the two components are different, growing as m_1/m_2 or σ_1/σ_2 up to a finite limiting value. In all cases, the component with larger m or σ moves to the cold. What is more striking, however, is that not only the amplitude, but also the *very existence* of thermal diffusion depends on the specific form of the interaction potential used for modeling collisions. Indeed, D_T is largest for hard spheres and decreases for softer repulsive potentials, actually vanishing for Maxwell's model potential $u(r) \sim r^{-5}$. Such a strong dependence is quite uncommon for kinetic transport coefficients. Quoting Chapman, thermal diffusion is therefore *'... one of the few properties of a gas which depends essentially on the particular characteristics of the molecules'*, that is, *'in its very nature (i.e., not merely in absolute magnitude) on a particular molecular model'*.

Purely kinetic theories are notoriously inadequate to describe liquids: nonetheless, some of the former features are shared by liquid mixtures. At least for liquids interacting via a Lennard-Jones potential, the sign of S_T and the molecular mass dependence of D_T agree with what is predicted for gases. For simple mixtures, the effects of attractive forces and of structural organization mirror into a qualitative correlation of thermal diffusion properties with the cohesive energy of the system, quantified by the Hildebrandt parameter [14]. For more complicated interactions, however, the situation is much more complicated: mixtures where hydrogen bond contributions are dominant, such as water + ethanol, display for instance a sign-reversal of S_T as a function of concentration.

Since analytical models of the Soret effect in liquids are far beyond the present capabilities of statistical mechanics, resorting to numerical studies seems to be unavoidable. Yet, simulation of non-equilibrium systems is far from being easy, and only recently have sophisticated numerical approaches such as non-equilibrium molecular dynamics (NEMD) been consistently established. Most of the studies so far performed have however concentrated on confirming basic experimental evidence, such as the tendency of the heavier species to move to the cold side (for a detailed review, see [14]). An interesting approach has been followed by Artola and Rousseau [15], who tried to extract a purely 'chemical' (interaction) contribution to the Soret coefficient by simulating mixtures of two components having the same mass and size, but different Lennard-Jones self-and cross-interaction parameters ϵ_{ij}. Their results are better discussed in terms of the dimensionless parameters $\psi_\epsilon = \epsilon_{11}/\epsilon_{22}$ and $k_{12} = \epsilon_{12}/\sqrt{\epsilon_{11}\epsilon_{22}}$. For $\psi_\epsilon = 1$, the Soret coefficient of component 1 is a linear function of the molar fraction x_1, switching sign from $S_T > 0$ to $S_T < 0$ when $x_1 = x_s \simeq 0.5$. In other words, the *less concentrated* component always goes to the cold side. The value of k_{12} only controls the limiting values for $x_1 = 0, 1$, and therefore the line slope. Much more interesting is the effect of increasing ψ_ϵ, which results in a concentration-independent downward shift of S_T, and therefore a substantial decrease in x_s. Besides showing that, in liquid mixtures, thermal diffusion may exist even for components with equal mass and size, this approach yields therefore very interesting qualitative information concerning the sign of S_T and its relation to specific molecular interaction parameters.

Although the theoretical understanding of the Soret effect in liquid mixtures is in general rather poor, there is an important exception. In liquid mixtures close to a critical point, the Soret coefficient diverges as $S_T \sim (T - T_c)^{-\nu}$, where $\nu \simeq 0.63$ is the usual critical exponent for the correlation length ξ. The divergence of S_T, originally observed by Giglio and Vendramini [16], has been explained by Mistura [17] by showing that it is only due to the critical slowing-down of D, while D_T is a regular, ξ-independent quantity remaining finite at $T = T_c$. This amounts to saying that D_T is related only to local, microscopic quantities, and is totally insensitive to the size of the correlated regions coherently driven by the thermal gradient.

2.2. Particle thermophoresis in gases

Thermally driven transport in aerosols has been known since the seminal observation by Tyndall [18] who, by visually observing the light scattered by hazes, noticed that the suspended dust particles tend to avoid hot surfaces. Although a deep connection to the Soret effect obviously exists, the theoretical analysis of particle thermophoresis in gases proceeded along a totally independent route (with the noticeable exception of the work by Chapman [19]).

The basic mechanisms underlying thermophoresis in gases are very different, depending on the ratio $Kn = \lambda/a$ between

the mean free path λ and the particle size a (the Knudsen number). When $Kn \gg 1$ (very low density gases), the problem is actually very similar to thermal diffusion in a gas mixture where one of the two components (the particles) has an exceedingly large size compared to the other. We are more interested in the opposite limit, $Kn \ll 1$ (gas at moderate pressure), which is properly called the 'quasi-hydrodynamic regime'. The basic ideas allowing us to understand thermophoresis in this regime stem from the last paper by Maxwell [20], where stresses in rarefied gases arising from inequalities of temperature are thoroughly investigated[5]. The key result of this paper is that, in a homogeneous gas, no longitudinal (pressure) or transverse stresses are associated with temperature gradients. The situation is however very different when a bounding solid surface is present. Let us indeed assume that the gas is bounded by a planar surface S, with a temperature gradient *parallel* to S, and consider those molecules that lie within a mean free path λ from S (and therefore suffer no molecular collision before hitting the wall). Since the impacting molecules are not specularly reflected (outgoing molecules have a partially random momentum distribution, due to thermalization with S), each molecule transfers a momentum Δp to the wall. A careful evaluation of the total momentum exchange requires however taking into account corrections to the equilibrium distribution $f_0(v)$ of the molecular speed, which *must* be included to account for dissipative processes. From the Boltzmann equation, one finds at first order [22]

$$f(v) = [1 + Cv_z(5/2 - mv^2/2k_BT)]f_0(v), \qquad (5)$$

m is the molecular mass, C is a normalization constant, and the thermal gradient is taken along z. If this is made, the total rate of momentum transfer turns out to be larger for those molecules coming from the hot side: therefore a net *longitudinal* momentum transfer takes place, pulling S towards the cold side.

Using Maxwell's result, Epstein [23] was able to calculate the steady-state thermophoretic velocity acquired by particle with thermal conductivity κ_p, embedded in a gas having thermal conductivity κ_g, viscosity η, and number density ρ:

$$v_T = \frac{3\eta}{2\rho T}\left(\frac{\kappa_g}{2\kappa_g + \kappa_p}\right)\nabla T_0. \qquad (6)$$

Since Epstein's seminal contribution, extensive theoretical and experimental work on thermophoresis in gases has been performed (as general reviews, see, for instance [24–26]), which even spurred the development of widely used thermophoretic soot sampling methods [27]. Furthermore, the intimate connection between thermophoresis and thermal diffusion in gas mixtures has been thoroughly investigated [28]. For our purposes, however, it is sufficient to stress some basic features of the mechanism driving thermophoresis in the quasi-hydrodynamic regime. (i) The gas exerts on the surface a purely tangential stress. Therefore, within a surface layer with a thickness of the order of λ, the pressure tensor is anisotropic. (ii) Because only *tangential* stresses are involved, even if it is a surface effect, the total force on the particle F_T scales only with a, and not a^2 (so that $v_T = F_T/f$, where f is the friction coefficient, is size independent[6]). (iii) In hydrodynamic terms, v_T can eventually be seen as a *slip* velocity of the particle, with a slip length $\ell \sim \lambda$. (iv) Particle *bulk* properties enter the problem only through the thermal conductivity κ_p, that, together with κ_g, determines the local temperature field around the particle via the heat equation.

2.3. 'Phoretic' phenomena in suspensions

Colloid thermophoresis is actually just a particular case of a larger class of transport effects collectively dubbed 'phoretic motion', whose specificity is to be essentially related to particle/solvent interfacial properties. The peculiarity of phoretic motion can be better appreciated by comparing them to a bulk transport mechanism such as sedimentation. In gravity settling, a particle is subjected to a force proportional to its buoyant mass, a bulk property scaling as the particle volume, which is balanced by the viscous drag scaling as the particle radius a. As a consequence v_S scales as a^2. Consider instead the case of electrophoresis. Each colloidal macroion is surrounded by an oppositely charged counterion cloud, fully screening the surface particle charge on a length scale of the order of the Debye–Hückel length λ_{DH}. An externally applied electric field 'sees' the overall particle + counterions system as electrically neutral: no 'bulk' driving force is therefore present. It is the *interfacial* motion and redistribution of the counterions that actually drives particle motion. As for thermophoresis in gases, particle motion can again be envisaged as a hydrodynamic slip effect. Here, the inhomogeneous region where the fluid velocity field $v(\mathbf{r})$ is non-zero is of the order of λ_{DH} (playing a role similar to λ for thermophoresis in gases). Due to their great practical interest, electrokinetic effects have been of course extensively studied. In general, the electrophoretic mobility is a complex function of the surface particle potential and solution ionic strength[7]. Here, we only recall that, in both limiting cases $\kappa a \gg 1$ and $\kappa a \ll 1$, where $\kappa = (\lambda_{DH})^{-1}$, the electrophoretic mobility does not depend on particle size, provided that the ζ-potential (the electrostatic potential at a distance from the particle surface where $v(\mathbf{r})$ is equal to the particle drift velocity) is constant.

Interfacially driven motion can however also be induced by different methods, for instance by creating gradients of pH, concentration of an osmolyte or, more generally, of the chemical potential of the solvent. These effects, collectively known as 'diffusiophoresis', differ from electrophoresis since they are non-equilibrium phenomena where no 'external field' is present. Nonetheless, they share the property of being essentially related to particle surface (not bulk) properties[8].

[5] Maxwell's paper accounts both for the 'radiometric forces' discovered by Crookes and for the 'thermal transpiration' effects observed by Reynolds. For a beautiful historical recollection, see [21].

[6] We point out that v_T does not depend on a also for $Kn \gg 1$. Dependence on particle size is present only for $Kn \sim O(1)$.

[7] For time-varying electric field, additional complex effects such as ion retardation and double-layer polarization make the analysis much harder.

[8] In spite of its name, dielectrophoresis, driven by the difference between solvent and particle dielectric constants, is not in this sense a phoretic effect (dielectrophoretic forces are indeed proportional to the particle volume).

In the past, noticeable attempts to give a general picture of phoretic motion have been made by Derjaguin [29] and Anderson [30]. Since phoretic motion is driven by interfacial stresses localized in a thin region of thickness δ close to the particle surface, calculation of the velocity field proceeds in general by determining the flow within this internal region, evaluating the slip at the particle surface, and plugging it as an effective boundary condition in the Navier–Stokes equations. A general conclusion which can be drawn by these approaches is that, provided $\delta \ll a$, the steady-state particle drift velocity does not depend on the particle size. This result is further supported by a recent general model of interfacial transport due to Ajdari and Bocquet [31].

Derjaguin and Sidorenkov [32] explicitly considered the case of thermophoresis (or, more precisely, the related effect of thermo-osmosis, i.e. thermally driven flow of liquids near solid surfaces), obtaining in the quasi-planar approximation $\delta \ll a$ a particle drift velocity

$$v_T = -\frac{2\nabla T}{\eta T}\int_0^\delta \Delta h(z) z \, dz, \tag{7}$$

where $\Delta h(z)$ is the solvent excess enthalpy due to interactions with the particle surface within the internal region. Although quite interesting in connection with the recent theoretical attempts presented in section 5, equation (7) cannot be easily compared to experimental results. A more interesting approach, giving an illuminating physical picture of phoretic effects, is due to Ruckenstein [33]. Noticing that in the limit of a $\lambda_{DH} \ll a$ and low surface potential the electrophoretic velocity v_E of a colloidal particle can be written as $v_E = (-\lambda_{DH}/\eta)\nabla\gamma$, where γ is the electrostatic contribution to the interfacial tension, Ruckenstein suggests that a similar expression for the steady-state drift velocity may hold for any kind of phoretic motion:

$$v_T \sim -\ell\nabla\gamma/\eta \tag{8}$$

where ℓ is a characteristic length of the order of δ. Phoretic motion is therefore envisaged as a kind of 'Marangoni effect' due to interfacial tension gradients caused by an external field (or composition, pH, temperature differences) in the diffuse inhomogeneous region close to the particle surface.

3. Experimental methods

The key reason for the recent noticeable increase of experimental investigations of particle thermophoresis in liquids has been the development of new, sensitive techniques, allowing us to obtain a rather large set of accurate data on different systems. In this section, we shall critically review these new techniques, describing their respective advantages and limits, but also pointing out the possibility of further developments.

Traditionally, the experimental methods for studying the Soret effect in binary liquid mixtures have been based on applying a thermal gradient to a suitable diffusion cell, and devising ingenious ways to detect the concentration gradients induced by thermal diffusion. In principle, the simplest way to do it would be placing the sample between two horizontal plates across which a constant temperature difference ΔT is maintained, and comparing the composition of the solution at steady state close to the two plates. However, the fractional separation of the components is generally small, and careful sampling of the local concentration presents non-trivial practical problems. Much better separation can be obtained by exploiting the concurrent action of thermal diffusion and buoyancy-driven convection in 'thermogravitational' columns [34], where a *horizontal* temperature gradient is imposed between two long vertical closely spaced surfaces, leading to the formation of a natural convection roll. Components that, because of thermal diffusion, preferentially drift to the cold (hot) plate become enriched at the bottom (top) of the column. This method (which was first tentatively used for isotope separation [35]) may lead to very high (even complete) component separation. Thermogravitational columns are however rather inefficient when dealing with colloidal suspensions, since, due to the very low diffusion coefficient of the solute, the timescale needed to obtain a sufficient separation ratio may be extremely long.

3.1. Optical probing: beam deflection methods

Optical probing of a concentration gradient is a very convenient way to overcome some of the basic limitations of the traditional methods. Provided that the refractivities of the particles and solvent are not exactly matched, a refractive index gradient ∇n is unavoidably associated with ∇c. Its noticeable effects on beam propagation allow measuring concentration differences which may be far smaller than those detectable by common analytic methods. More important, probing is carried out *in situ* (does not require any sampling), and absolute values for S_T can often be obtain by direct comparison with optical effects on the pure solvent, with no reference to the specific apparatus geometry. Finally, using moderately focused laser beams, thermal gradients can be imposed on spatial scales which are rather small (although not *very* small), yielding shorter measurement times than with thermogravitational columns.

All these positive features are fully exploited by the simple but powerful 'beam deflection' method (BD), originally developed by Giglio and Vendramini, which takes advantage of the deflection of a laser beam propagating along the horizontal direction $\hat{\mathbf{x}}$ through an optically inhomogeneous medium with $\nabla n = (dn/dz)\hat{\mathbf{z}}$. The investigated solution is enclosed in a cell made of an optical glass frame sandwiched between two horizontal thermally conducting plates separated by a small vertical gap h. When a small temperature difference is rapidly imposed between the two plates, the beam undergoes a first rapid angular deflection $(\Delta\vartheta)_{th}$ due to the temperature dependence of the solvent refractivity, followed by a much slower change $\Delta\vartheta_s(t)$ due to progressive buildup of the concentration gradient associated with thermophoresis, eventually leading to an additional steady-state deflection $(\Delta\vartheta)_s$. The two contributions are easily discriminated since they are widely separated in timescales, respectively set by the solvent thermal diffusivity χ_T and by the particle diffusion coefficient, with $\chi_T \gg D$. To measure beam deflection, a

position-sensitive detector is usually placed along the beam path sufficiently far from the cell. The Soret coefficient is simply evaluated as

$$S_T = -\frac{1}{c}\frac{\partial n/\partial T}{\partial n/\partial c}\frac{(\Delta\vartheta)_s}{(\Delta\vartheta)_{th}}, \quad (9)$$

where $\partial n/\partial T$ and $\partial n/\partial c$ are respectively the temperature and concentration dependence of the refractive index. In addition, the time dependence of $\Delta\vartheta_s(t)$, which reaches its steady-state value exponentially with a time constant $\tau = h^2/(\pi^2 D)$, allows evaluation of the particle diffusion coefficient, and therefore $D_T = S_T D$.

The BD technique, besides being conceptually and practically very simple, has the key advantage of exploiting an intrinsically differential detection scheme. Equation (9) indeed shows that S_T can be obtained by comparison to the pure 'thermal' deflection contribution knowing only the values of $\partial n/\partial T$ and $\partial n/\partial c$, with no need to use any geometrical or optical parameter of the specific experimental setup. As a matter of fact, it is not even necessary to calibrate the system with the sample which is actually investigated, since it is sufficient to measure $(\Delta\vartheta)_{th}$ for *any* reference solvent. Finally, since for the typical values of the interplate gap the threshold for the Rayleigh–Benard convection of the pure solvent is very high, both the top and the bottom surfaces can be used as the hot plate, the latter choice being mandatory for $S_T < 0$ to avoid the much more serious convection problems generated by inverted concentration profiles.

The main limitation of the BD method is that the interplate gap h cannot be reduced below a minimal value of the order of a few tenths of a millimeter. This is not so much due to practical construction problems, but rather to the fact that the beam cannot be focused within the cell to an arbitrarily small spot size w_0. In order to have a well defined beam propagation direction, indeed, the cell optical path L has to be sensibly shorter than the Rayleigh range of the focused beam $z_R = \pi w_0^2/\lambda$. For a wavelength $\lambda \simeq 0.5$ μm, a cell with an optical path of a few centimeters requires $w_0 \geqslant 100$ μm, corresponding, to avoid reflections, to a 'safe' interplate gap $h \simeq 0.3$–0.4 mm. With such a gap, the diffusion time for a suspension of colloids with radius $R \simeq 10$ nm is already $\tau \simeq 10^3$ s, so that measuring thermophoresis of large colloids is time consuming and requires very accurate temperature control. A second limitation is that, to avoid the deflected beam impinging on the top or bottom plate, the overall beam deflection angle must satisfy $(\Delta\vartheta)_{th} + (\Delta\vartheta)_s \ll h/L$. When $(\Delta\vartheta)_{th}$ is already large, the maximum temperature gradient which can be imposed can be rather small. Therefore, BD works much better with aqueous suspensions (due to the rather low thermal expansivity of water) than with particle dispersed in organic solvent, where $\partial n/\partial T$ can be much higher.

An attempt to overcome the geometrical limitations of BD has been made by Putnam and Cahill, who have designed a 'micro' BD apparatus [36]. In this setup, temperature gradients are produced by alternately heating with a square-wave voltage signal a pair of Au thin-film resistors fabricated by photolithography on a glass substrate, allowing us to reduce the plate separation to 25 μm. Since the optical path is very small (the electrodes are only 250 μm thick), detection is made in the frequency domain via a sensitive lock-in amplifier, allowing us to obtain both the in-phase and out-of-phase components of the BD signal. This ingenious approach allows us to reduce substantially the time duration of BD experiments, although, when the frequency of the applied T-signal is very low, rather long accumulation periods are still needed.

3.2. All-optical methods

A very efficient reduction of the spatial region where particle diffusion is probed, and therefore of the measurement time, can be obtained by inducing localized thermal gradients via laser beams. This can be done either by exploiting a moderate optical absorption of the sample at the frequency of the incoming beam, or by adding a small quantity of a suitable dye acting as an absorber. In one of these techniques, thermal lensing, which we shall consider in more detail, the beam acts at a same time as a 'pump' and as a 'probe'. Other schemes, which we shall review only briefly, either use an additional probing beam, or rely on the detection of the fluorescence signal from suitable particles. At variance with BD methods, these all-optical methods do not require any complicated custom-designed cell, and, at least in the case of thermal lensing, can be implemented with a simple optical design. On the other hand, all-optical methods require careful consideration of spurious convection problems, which can seriously limit their performance.

3.2.1. Thermal lensing. Thermal lensing (TL) is a self-effect on beam propagation taking place when a focused laser beam heats up a partially absorbing medium, generating a locally inhomogeneous refractive index profile [37]. Thermal expansion indeed induces a radial density gradient, which in its turn yields a quadratic refractive index profile acting as a negative lens that increases the divergence of the transmitted beam. Beam widening can be very accurately measured by detecting changes of the central beam intensity, a feature that makes TL suitable for absorption measurements in simple fluids with extinction coefficients as low as 10^{-7}. For this reason, TL has been established as a highly sensitive technique for trace analysis in chromatography and electrophoresis, both in its basic configuration and in more sophisticated instrumentation design including double beam, differential, spectrally tunable setups [38].

Besides its excellent performance as a spectroscopic method, TL can be profitably exploited for investigating thermophoresis. Indeed, in fluid mixtures or suspensions, thermal diffusion also leads to the progressive buildup of a *concentration* gradient within the heated region, which acts as an additional lenslike element. This 'Soret lens' can be either divergent or convergent, depending on the preferential drift direction of the component having the largest index of refraction. As a result, the spreading of the transmitted beam may further increase, or conversely lessen. As for BD, 'thermal' and 'Soret' lensing effects take place on widely separated timescales, due to the different order of magnitudes of thermal diffusivity and mass diffusion. The first

application of thermal lensing to thermal diffusion was made again by Giglio and Vendramini [39], who measured thermal diffusion close to a critical point in the strongly absorbing aniline/cyclohexane mixture. Aqueous colloidal suspensions, however, generally present negligible absorption in the visible range, so that, to obtain a significant TL signal, absorbing dyes are often added. Yet, extreme attention must be paid to avoid dye bleaching or preferential absorption on the particle surface. Moreover, dye molecules are often charged, limiting therefore the lowest ionic strength that can be attained for charged suspensions. An alternative strategy is that of directly exploiting water absorption in the near infrared, for instance at $\lambda \simeq 980$ nm, due to combinations of vibrational overtones. A practical additional advantage is that reliable, tunable, and relatively inexpensive semiconductor laser sources have been developed in this wavelength range due to its interest for optical communications.

We shall only recall only those theoretical results for TL that are experimentally most relevant, deferring the reader to the comprehensive analysis performed in [40] for further details. The 'purely thermal' and 'Soret' contributions to the beam divergence are respectively related to the dimensionless 'thermal lens numbers'

$$\begin{aligned} \vartheta_{\mathrm{th}} &= -\frac{Pbl}{\kappa\lambda}\frac{\partial n}{\partial T} \\ \vartheta_{\mathrm{S}} &= \frac{Pbl}{\kappa\lambda}\frac{\partial n}{\partial c}S_{\mathrm{T}}c(1-c) \end{aligned} \tag{10}$$

where P is the optical power of the beam incident on a sample with thermal conductivity κ and absorption coefficient b, and l is the optical path length. Provided that $\vartheta_{\mathrm{th}}, \vartheta_{\mathrm{S}} \ll 1$, the Soret coefficient can be extracted by a comparison of the steady-state total change of the intensity at the beam center $\Delta I_{\mathrm{S+th}}$ to the change purely due to the thermal expansion of the fluid ΔI_{th} as

$$\frac{\Delta I_{\mathrm{S+th}}}{\Delta I_{\mathrm{th}}} = 1 - S_{\mathrm{T}}\bar{c}(1-\bar{c})\frac{\partial n/\partial c}{\partial n/\partial T}, \tag{11}$$

which parallels the expression obtained for the BD method. An important experimental aspect of the BD technique is that the signal strongly depends on the position of the cell with respect to the beam focus. In particular, the TL effect vanishes if the cell is placed exactly at the beam waist while, if one takes into full account lens aberration effects using a full diffraction analysis, the effect is maximized by placing the cell at a distance $z = \sqrt{3}z_{\mathrm{R}}$ from the focus[9].

The crucial problem in TL measurements is that radially symmetric beams necessarily generate a *horizontal* component in the temperature gradient, and therefore free convection is *unavoidably* present, regardless of the chosen experimental configuration. For simple fluids, the disturbance of the density profile (developing on a timescale set by the heat diffusivity χ) due to convection effect is minimal, and has therefore generally been disregarded. The situation of totally different for the concentration gradient induced by thermal diffusion, whose characteristic buildup time is fixed by D. The basic strategy to limit convection effects is reducing the measurement duration so much that, on the required experimental timescale, perturbations of the concentration profile are negligible. This can be safely obtained by placing the optical axis of the apparatus vertically (which allows use of cells with a short optical path, therefore limiting the vertical height over which buoyancy acts), or by sufficiently focusing the incident beam. Strong beam focusing, however, severely reduced z_{R}, and therefore the maximum useful optical path length.

When compared to the BD method, TL allows studying suspensions of particles with a much bigger size. For small particles, the accuracy of the values for S_{T} obtained with the two methods is comparable, although BD generally yields more accurate values for the diffusion constant, and therefore for D_{T}. Obviously, TL would perform almost ideally in the absence of gravity, so that, due to its extreme optical simplicity (essentially a laser source, an electro-mechanical shutter, a focusing lens, a standard cuvette, and a photodiode) it is an extremely promising technique to measure thermophoresis in space.

3.2.2. 'Thermal diffusion' forced Rayleigh scattering (TDFRS). This approach bears many points in common with similar techniques, commonly (but rather improperly) dubbed 'forced Rayleigh scattering' (FRS) methods, which are used, for instance, in hydrodynamic flow visualization, particle velocimetry, or colloidal electrophoresis. Basically, they consist in reading, via a probing beam, the transient diffraction grating created in a sample by two mutually coherent excitation ('pump') beams propagating through the sample with slightly different incident wavevectors. If the pump wavelength is partially absorbed by the fluid or, as more commonly made, if a suitable absorbing dye is added to the sample, a diffraction grating, due as in the TL method to the temperature dependence of the refractive index, builds up on a timescale set by the thermal diffusivity. In the presence of thermal diffusion, the associated sinusoidal temperature field leads to the progressive buildup of a concentration gradient, which in turn modifies the refractive index profile, changing the grating diffraction efficiency, whose time dependence is read by measuring the intensity of the Bragg-diffracted probing beam [41]. As in the TL method, the measurement scheme is intrinsically differential. Another advantage of TDFRS is that only the Fourier component at the grating wavevector contributes to the signal, which allows for an easier de-convolution of multiple decay functions obtained for polydisperse colloids or polymer solutions with a large M_w distribution. However, also for TDFRS, inverted temperature gradients and therefore convection effects are unavoidable. In principle, these effects can be limited very easily by increasing the spatial frequency of the grating, which is fixed by the crossing angle θ between the pump beams. In practice, however, large values of θ, besides requiring the grating to be treated as a fully three-dimensional holographic pattern

[9] Measurements of TL signals can also be made by recording the full dependence of the central beam intensity as a function of the cell position z. Although necessary for setup calibration, however, this protocol (commonly dubbed 'z-scan') does not add any new information in comparison to simpler measurements made with a cell fixed in the position where the signal is maximal.

using the rather complex Raman–Nath theory, generally lead to a substantial reduction of the diffraction efficiency. An interesting alternative method to easily generate diffractive concentration gratings with high spatial frequency has been recently proposed by Hartung and Köhler [42]. In this setup, a linear array of transparent ITO (indium tin oxide) strips, sputtered on the inner window of the measuring cell, can be electrically heated to create a periodic temperature modulation, while detection of the associated Soret-induced concentration gradient is pretty similar to standard TDFRS. This new method, which bears some similarity to the approach taken in [36], may potentially retain the advantages of all-optical methods, while at the same time benefiting from a well defined thermal geometry with negligible convective effects.

3.2.3. Fluorescence detection schemes and single-particle tracking. Spurred by great advancements in optical microscopy, such as confocal detection schemes and advanced particle-tracking methods, direct visualization of colloidal particles has became more and more popular in the last decade. It is therefore tempting to see whether studies of thermophoresis could be performed using 'standard' video microscopy instrumentation and techniques. The basic strategy of this approach, which has been mainly followed by Braun and coworkers [43], consists (as in TL) in inducing a very localized thermal gradient by the adsorption of a laser beam, using however simple cells, built from microscopic slides or capillaries, and standard microscope optics. Using fluorescent-dyed particles, the concentration profile can be reconstructed by monitoring through the microscope the spatial and time dependence of the fluorescence intensity. The major advantage of this method is that of exploiting standard fluorescence microscopy instrumentation and techniques, with no need for specific optical schemes or custom-designed cells. Fluorescence detection methods are moreover so sensitive that even extremely particle low concentrations can be measured. There are obviously also disadvantages. First of all, the method works only for particles that are intrinsically fluorescent, or made such by adsorption of a dye. Moreover, absolute fluorescence intensity measurements are also notoriously hard, due to the difficulty of quantitatively taking into account dye-bleaching effects. Finally, monitoring the temperature field is non-trivial. Braun and coworkers have developed the ingenious strategy of using as a temperature probe a dye whose fluorescent emission is temperature dependent. Nonetheless, the sensitivity of this probe is rather low (a few per cent per degree), so that much higher temperature gradients are needed than those used in TL measurements. But the key advantage of the method is that, provided that particles are sufficiently big that individual particle emission is resolved, colloid thermophoretic motion can be directly visualized. For suspensions of very large particles (say, in the few μm range), where even all-optical techniques become unbearably slow, single-particle tracking by fluorescence microscopy is currently the only method to obtain v_T, and therefore D_T. It is useful to consider the role of the characteristic length ℓ_T in particle-tracking experiments. For the contribution of thermophoretic drift to be an appreciable fraction of the particle rms displacement, the latter has to be comparable to ℓ_T. The minimum tracking time will therefore be shorter for very large particles or high thermal gradients.

4. Experimental results

4.1. A survey of investigated systems

4.1.1. Colloidal latex particles. Suspensions of rigid, monodisperse spherical particles have traditionally been the 'test bed' for colloid physics. One may therefore regard them as the best candidate to investigate the basic mechanisms of thermophoresis: the experimental status is conversely rather disappointing. Indeed, thermophoresis seems to strongly depend on detailed surface chemistry properties. For instance, polystyrene (PS) and silica particles of similar size and surface charge, in ionic strength conditions where they can be regarded just as 'hard spheres' as concerns colligative properties, may display a Soret coefficient of opposite sign. Besides, adsorbing a thin layer of surfactant or grafting a short polymer chain may lead to dramatic changes in S_T. Unfortunately, the surface chemistry of 'standard' colloidal latices is far from being standardized. The bare particle charge Q cannot be carefully controlled, stated charge values should be taken with great care (for large colloids, careful charge titration is difficult), and electrokinetic parameters such as the ζ-potential are not easily related to Q. The surface properties of inorganic particles such as silica colloids strongly depend on pH and, for commercial silica, on the presence of 'stabilizing' counterions. Residual surfactant is often present on the surface of polymer latex colloids obtained by emulsion polymerization, even when the batches are sold as 'surfactant-free'. An additional practical problem is that most experimental methods perform better with suspension of particles of relatively small size (say, tens of nanometers), notoriously hard to obtain with a narrow size distribution.

Nonetheless, in the last few years a number of interesting studies have been performed on dispersions of monodisperse colloidal particles. An extensive study of polystyrene suspensions as a function of (nominal) surface charge, pH, ionic strength, and nature of the added salt has been performed by Putnam and Cahill [36]. PS particles have been used also by Duhr and Braun [44], and more recently by Braibanti *et al* [45] to investigate some basic features of particle thermophoresis, such as the dependence on particle size and temperature. Nonaqueous suspensions of sterically stabilized silica particles, where the particle/solvent interaction potential is tuned by temperature, have been studied by Ning *et al* [46]. The results of these studies will be analyzed in the next section. Other measurements, in particular in ferrofluids, where complex cross-effects of thermal gradients and magnetic fields are observed [47], have been mostly performed using rather polydisperse suspensions. Taking into account the specific purpose of this review, aimed only to scrutinize the basic mechanisms of thermophoresis, they will not be further discussed in what follows.

4.1.2. Surfactant aggregates. Studies of micellar solutions formed by surfactant molecules in water provide in our view a unique occasion to understand the role of particle/solvent interactions in thermophoresis, due to the broad class of very different amphiphilic molecules that can be investigated. Varying the chemical nature of the hydrophilic head group exposed to the solvent (simple or aromatic salts, carboxylic acids, zwitterionic amino acids, fatty alcohols, polyoxyethylenes, sugars, to cite a few) allows us indeed to obtain widely different interaction forces with the solvent. Globular micelles are moreover small colloids, in the few nanometers range, which do not require long measurement times and are less sensitive to spurious convection effects. Finally, the micellar structure can often be drastically changed by varying the solvent composition, surfactant concentration or temperature, allowing us to investigate effects on thermophoresis of structural re-organization phenomena. A first detailed investigation of a micellar solution of sodium dodecyl sulfate (SDS), where some of the general features of thermophoresis we shall discuss were first observed, has been performed by Piazza and Guarino [48]. The same group then studied thermophoresis in mixed micelles or ionic and sugar surfactants [49]. Nonionic polyethylene glycol surfactants, which generally display a critical consolution point with water, have been investigated by Ning *et al* [50]. Nonetheless, considering the promise of micellar solutions as model systems, the number of investigated systems is still very limited. This is yet more true when taking into account that amphiphilic molecules are the building blocks of other interesting structures besides micelles. For instance, thermodynamically stable water-in-oil (W/O) or oil-in-water (O/W) microemulsion droplets, whose size can often be carefully tuned in a moderately large range, can form in ternary water + oil + surfactant solutions. So far, the only investigated system has been AOT/iso-octane/water W/O microemulsions [51]. Double-chain amphiphiles such as phospholipids can also form large, monodisperse vesicles, which could be an interesting candidate to investigate cell thermophoretic migration. It is therefore evident that further investigation of amphiphilic systems is sorely needed.

4.1.3. Proteins and biological macromolecules. As we shall see, the peculiar temperature dependence of aqueous colloid thermophoresis allows design of new fractionation methods relying on particle/solvent interfacial properties. Given the current pressing demand for new separation techniques, the study of thermophoretic effects in biology-related systems may have useful consequences for applications. There are however also basic motivations for investigating biological macromolecules. Globular proteins are small colloids presenting peculiar features that allow investigation of a number of interesting aspects of particle thermophoresis in liquids. Their net charge, stemming from the dissociation balance of acid and basic groups, can indeed be carefully trimmed by varying the solution pH. Moreover, their water-exposed surface may be envisaged as a 'tartan' made of hydrophilic and hydrophobic patches. Due to the complex nature of hydrophobic effects, protein interactions with water strongly depend on temperature, and very strong salt-specificity effects on solubility are observed. So far, thermophoresis in protein solutions has been studied only for a few simple proteins like lysozyme [52] and β-lactoglobulin [49]. The few existing studies of DNA thermophoresis [53, 43] have shown that the concurrent action of thermophoresis and convection may lead to a noticeable DNA focusing effect of possible interest as a biochemical concentration method. As for surfactants, there are therefore ample margins for the study of thermophoresis in biology-related systems.

4.1.4. Polymers. Polymer physics is notoriously the most advanced field in soft matter science. It is therefore not surprising that great experimental and theoretical efforts have already been devoted to understand thermal diffusion in polymer solutions (actually, till the end of the last century, polymers have practically been the *only* investigated soft matter system). Since thermal diffusion in polymer solutions has recently been reviewed [14], we only discuss here some selected theoretical and experimental results that may be useful for what follows.

The main theoretical prediction concerning polymer thermophoresis is that D_T should not depend on the molecular weight M_w. The original idea, due to Brochard and De Gennes [54], is not so much based on scaling considerations, but rather on a clever combination of non-equilibrium thermodynamics and hydrodynamic concepts. Their argument, quite often misreported, can be sketched as follows. Consider a polymer simultaneously subjected to a thermal gradient *and* to an arbitrary external field $\mathbf{f}$. Due to Onsager reciprocal relations, the thermophoretic contribution to the polymer drift velocity (which adds to the value $\mathbf{v} = \mathbf{f}/f$ for $\nabla T = 0$) must equal the contribution of $\mathbf{f}$ to heat transport. The latter can be written as the sum of a term J_1 proportional to the friction on each monomer plus a hydrodynamic term J_2 related to $\nabla^2\mathbf{v}_s(r)$, where $\mathbf{v}_s(r)$ is the solvent velocity field. Their key result is that, because for Stokes flow $\nabla^2\mathbf{v}_s(r)$ is very short ranged, J_2 leads only to a 'renormalized' value for J_1. In other words, long-ranged hydrodynamic interactions, playing a crucial role in fixing f, have conversely no effect on heat transport. As a consequence, the 'reciprocal' heat flux is simply proportional to the number of monomers, and D_T does not depend on M_w. Experimentally, this results has been extensively verified for sufficiently long chains both in dilute [55, 56] and semidilute [57] polymer solutions[10]. The situation may be very different for charged polymers. In a preliminary study of a solution of sodium polystyrene sulphonate (NaPSS) in water, Iacopini *et al* [49] found that D_T actually *decreases* (approximately as $D_T \sim M_w^{-1/4}$) with the molecular weight of the polyelectrolyte. Long range electrostatic interactions seem therefore to introduce those inter-monomer correlations for D_T which are not brought by hydrodynamic effects.

Besides molecular weight effects, however, there are other aspects of polymer thermal diffusion that would deserve to

[10] Accurate studies of PS in toluene [58] have however shown that, due to end-effects, M_w-independence breaks down for $M_w < 5 \times 10^3$.

Table 1. Values of $\tilde{D}_T$ and D for some selected colloidal systems.

System	$\tilde{D}_T$ (10^{-6} cm^2 s^{-1})	D (10^{-6} cm^2 s^{-1})	Ref.
SDS	12.8	1.0	[48]
Triton X100	7.45	0.58	[45]
NaPSS ($M_w = 74$ kDa)	7.15	0.53	[49]
PS spheres ($R = 53$ nm)	4.7	0.03	[45]
PS spheres ($R = 253$ nm)	4.3	0.007	[45]

be investigated, such as the dependence of D_T and S_T on the specific physicochemical properties of the solvent. A quantitative analysis of solvent effects has been performed by Hartung *et al* [42], who have measured thermal diffusion of PS in seven different solvents. The main result of this investigation is that D_T is inversely proportional to the solvent viscosity (and, therefore, S_T does not depend on η). Recently [59], the same group has extensively investigated semidilute and concentrate polymer solutions, finding that the concentration dependence of D_T closely parallels that of the solvent self-diffusivity D_s^s. Since D_s^s may be viewed as a local probe for friction on a length scale of a polymer segmental unit, they argued that local friction is the dominating parameter determining the concentration dependence of D_T. Conversely, at least for polystyrene, D_T seems to be very little affected by the kind of solvent quality. Yet, a detailed analysis of possible correlations between D_T and the Flory parameter χ, which quantifies the 'quality' of the solvent, is still lacking, with the only possible exception of measurements performed in the vicinity of the coil-to-globule transition of poly(*N*-isopropylacrylamide) in water [60], showing that, by approaching the polymer θ-temperature, S_T first displays a moderate increase, followed by a sharp reduction of a factor of five when water becomes a bad solvent.

4.2. Some general experimental features

4.2.1. Specificity and universality. Thermophoresis in liquids displays a curious two-faced nature. On the one hand, the order of magnitude of D_T is rather 'universal'. For most investigated systems, the thermophoretic mobility varies indeed within the fairly limited range $10^{-8} < D_T < 10^{-7}$ cm^2 s^{-1} K^{-1}. For example, we have collected in table 1 some selected values of the 'rescaled' thermal diffusion coefficient $\tilde{D}_T = T D_T$ for aqueous systems ranging from micellar solutions to polymers and spherical latex particles. Strikingly, while D varies by more than two orders of magnitude, $\tilde{D}_T$ changes by no more than a factor of three. Notice also that, for large colloids, $\tilde{D}_T \gg D$, so that for equal fractional concentration and temperature gradients $\nabla c/c$, $\nabla T/T$, thermal diffusion is dominant. On the other hand, the variation of D_T among different colloidal systems cannot be easily related to simple bulk or surface particle properties (with the trivial exception of the difference in thermal conductivity with the solvent, which sets the local temperature field). Such a baffling feature is fully evidenced by the extensive investigation of PS colloids by Putnam and Cahill [36], where the value or even the sign of S_T were found to strongly depend on the kind of the surface charged groups and buffering conditions, while ionic strength effects display a marked salt-specificity. The strict relation between thermophoresis and the detailed nature of particle/solvent interactions has been fully evidenced in measurements of solutions of SDS + dodecylmaltoside (DM) [49]. By varying the relative weight fraction of the two surfactants, which form almost ideal mixed micelles, S_T can indeed be varied continuously between the limiting values (of opposite sign) for the pure compounds.

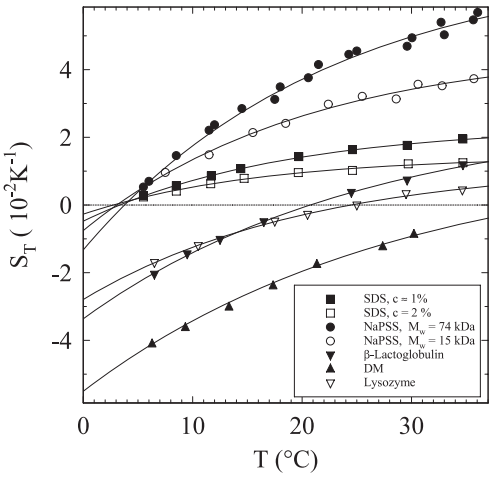

Figure 1. Temperature dependence of the Soret coefficient for some aqueous colloidal systems, fitted using equation (12). Detailed experimental conditions are given in [49].

4.2.2. Temperature dependence. Thermophoresis often displays a strong dependence on temperature, which was originally singled out for protein solutions [52], and later observed for many other aqueous and nonaqueous colloidal systems [49, 61–63]. The general temperature trend is the following: particles diffuse to the cold for sufficiently high temperatures, while $S_T < 0$ (so that particles display a 'thermophilic' behavior) below a well defined temperature T^*. The full temperature dependence of $S_T(T)$ is generally very well described by the empirical fitting function [52]:

$$S_T(T) = S_T^\infty \left[1 - \exp\left(\frac{T^* - T}{T_0}\right)\right], \qquad (12)$$

where S_T^∞ represents a (positive) high-T asymptotic limit, and the rate T_0 of exponential growth embodies the strength of temperature effects. A closer look at representative data sets, taken from [49] and shown in figure 1, allows extraction of some general features of the temperature dependence of S_T. First of all, we noticed that, for some systems that we shall dub 'athermal', T^* approximately coincides with the temperature where water has its maximal density. Moreover, the results obtained for NaPSS and SDS respectively suggest that T^* depends neither on the polymer molecular weight, nor on interparticle interactions. The value of the sign-switching temperature seems therefore to be a single-particle property that does not depend on particle size. For other systems, however, T^* can be very different. For instance,

surfactants such as DM, having a sugar head group, have a much higher value of T^*, therefore displaying at room temperature a thermophilic behavior. It is also useful noticing that the two investigated protein solutions display different values for T^*. In principle, therefore, a mixture of lysozyme and β-lactoglobulin could be fractionated by thermophoresis.

For 'athermal' systems (mostly colloidal solutions where the particle/solvent interactions are predominantly electrostatic), $S_T(T)$ closely mirrors the temperature dependence of the thermal expansivity of the solvent, $\alpha(T) = -1/\rho(d\rho/dT)$. Indeed, the dimensionless 'rescaled' Soret coefficient $\tilde{S}_T = S_T/\alpha(T)$ does not appreciably depend on T. For other systems, however, the relation between S_T and $\alpha(T)$ is not so simple and, to fit the data, a temperature-independent 'excess' contribution S_T^{exc} has to be introduced, writing $S_T = \alpha(T)\tilde{S}_T + S_T^{exc}$. Although the temperature effects we have discussed are rather general, we point out that, for a few aqueous systems such as poly-ethyleneglycol (PEG) solutions, S_T shows a very weak dependence on T (curiously, PEG conversely shows a pronounced T-dependence in water/ethanol mixtures) [64].

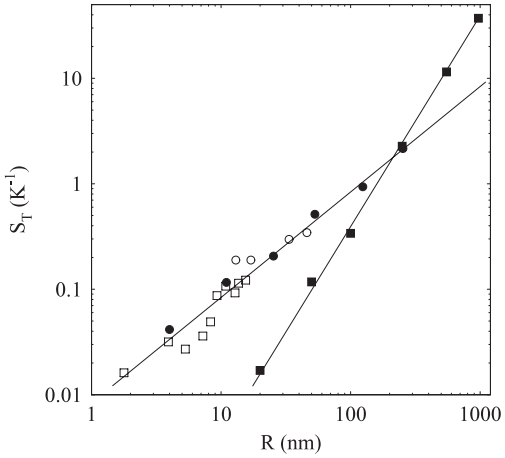

Figure 2. Size dependence of the Soret coefficient for PS colloids obtained by Duhr and Braun [44] (■), Braibanti *et al* [45] ($T = 35\,°C$, ●), and Putnam and Cahill [63] (S_T^∞, ○), together with values obtained for AOT W/O microemulsions by Vigolo *et al* [51] (□).

4.2.3. Particle size dependence. How do S_T and D_T depend on the particle size a? We should be a bit careful in posing this question, since interparticle interactions will in general introduce additional length scales besides a. Here we shall focus only on situations where the range of particle/solvent interactions is much shorter than a, which is therefore the only relevant length in the problem. Apparently, some of the topics we have discussed already give strong hints for a solution. In the quasi-hydrodynamic limit, the particle thermophoretic velocity in gases, and therefore D_T, does not depend on a. General arguments on colloidal 'phoretic' motion lead to the same conclusion. Finally, D_T does not depend on the molecular weight (and therefore on the hydrodynamic radius of the coil) for dilute solutions of polymer chains, which can in all respects be regarded as 'soft' globular colloids. Therefore, a size-independent thermophoretic mobility D_T (implying $S_T \propto a$) should also be reasonably expected for rigid colloids. Assuming $D_T \propto a^s$ with $s > 0$ also leads to unphysical consequences when we consider the reciprocal effect of thermo-osmosis, i.e. the flow of a liquid past a surface along which a longitudinal thermal gradient is maintained. Since the thermophoretic velocity is simply related to the thermo-osmotic velocity $\tilde{v}$ of the fluid by the reciprocal theorem for low Reynolds-number hydrodynamics [65], $\tilde{v}$ would indeed diverge for a flat surface. A size-independent thermophoretic mobility has actually been found for water-in-oil AOT microemulsions where the microemulsion droplet radius R was varied between 2 and 15 nm by changing the water/surfactant ratio [51]. For aqueous suspensions of rigid colloids, the status of the experimental results is however more controversial. Investigating PS latex colloids covering more than two decades in a, Duhr and Braun [44] rather concluded that $D_T \propto a$ and $S_T \propto a^2$. This conclusion has however been questioned by Putnam *et al* [63], who detected relevant temperature effects for the same system, and found that the high temperature limit S_T^∞ rather scales *linearly* with a. The latter result has been recently confirmed by Braibanti *et al* [45], who actually showed that, provided that the particle surface properties are carefully 'standardized', particles with a diameter $20 \lesssim a \lesssim 500$ nm very closely share the same $D_T(T)$ over the *whole* temperature range $5\,°C \leqslant T \leqslant 40\,°C$. No sound explanation of this serious experimental discrepancy has so far been suggested. Here we simply recall that, for the measurements presented in [44], data fitting seems to imply a T-independent value of S_T, although temperature differences as large as $\Delta T \simeq 8$ K were applied: conversely, both the data reported in [63] and in [45] suggest that S_T can vary by more than 50% within a similar T-range. Data sets for the size dependence of S_T in PS suspensions are collected in figure 2, together with the results obtained in [51] for AOT microemulsions. Curiously, the latter show not only the same general trend, but also absolute values that are close to those found for rigid colloidal particles.

4.2.4. Electrostatic interactions. Screened Coulomb interactions may noticeably influence thermophoresis and complicate the analysis, since the Debye–Hückel screening length λ_{DH} represents a new intrinsic length scale beside a. The strong contribution of electrostatic forces to S_T has been pointed out for the first time in the experiments performed on SDS solutions [48], where conspicuous collective effects due to the micellar charge were also observed (see below). By extrapolating S_T to the zero-concentration limit, Piazza and Guarino suggested that, in the single-particle limit, $S_T \propto \lambda_{DH}^2$. As we shall see in section 5.5, this scaling relation is strongly debated. Unfortunately, quantitative studies on other ionic surfactant systems, which may help in settling the question, are still lacking. One of the difficulties in dealing with micellar solutions is that the critical micellar concentration (c.m.c.) of charged surfactants is generally rather high, in particular in the absence of added salt, so that a non-negligible amount of free (non-micellized) surfactant, which contributes to the solution ionic strength I, is generally present. Stating an accurate value for λ_{DH}^2 is therefore a delicate problem.

A few charged surfactants with a very low c.m.c. (mainly because of their very large head groups) exist, but they are quite difficult to obtain in sufficient amount (and are therefore very expensive). Another candidate to investigate electrostatic effects is solutions of globular proteins, offering in addition, as we discussed, the opportunity of tuning the particle charge. So far, however, studies of protein solutions have been limited to rather large values of I (mainly because of the need of buffering the solution), where electrostatic effects are found to be rather weak [52]. As already discussed in 4.1.1 and 4.2.1, the situation is much more controversial for rigid colloidal particles. Here we only notice that, for big particles, charge effects may generally be expected to be much weaker, since both their surface charge density and the maximum achievable value of the ratio λ_{DH}/a are usually much smaller than for suspensions of small colloids.

4.2.5. Collective effects. As we shall see in section 5, developing a consistent model for the thermophoresis of a single colloidal particle, capable of accounting for the main experimental observations we have just discussed, is far from being easy. Working out a complete theory, taking into account also collective properties, may therefore seem a formidable task. Yet, the contribution of interparticle interactions to thermophoresis may be qualitatively simpler to gather than single-particle effects. It is therefore worth recalling some experimental results concerning the dependence of S_T and D_T on particle concentration. Striking collective effects on thermophoresis were originally singled out in [48]. Indeed, while in the dilute limit S_T grows with λ_{DH}, electrostatic intermicellar interaction leads, even at moderately low SDS concentration, to a totally reversed behavior, so that S_T actually *increases* with increasing salt concentration. A quantitative analysis of collective effects, made via a virial expansion, suggests S_T to be proportional to the osmotic compressibility $k_T = [n(\partial\Pi/\partial n)]^{-1}$ of the solution, where n is the particle number density. In [48], this relation was accounted for by assuming D_T to be insensitive to structural properties, and observing that D depends on k_T through the generalized Stokes–Einstein relation. Qualitatively, it is simple to see why S_T should be related to k_T: repulsive interparticle forces (low k_T) hinder the buildup of concentration gradients, whatever their origin, while, conversely, attractive interactions promote them. More quantitatively, assume that the effect of the thermal gradient on a single particle may be considered as equivalent to those of an effective external force $F^{\text{eff}} = K\nabla T$. The steady-state condition will therefore be $\nabla\Pi(c, T) = -K\nabla T n$, where Π may explicitly depend on T when interparticle forces are temperature dependent. Assuming ∇T directed along $\mathbf{z}$, we get

$$S_T = -\frac{1}{n}\frac{dn}{dT} = nk_T\left[K + \frac{1}{n}\frac{\partial\Pi}{\partial T}\right]. \tag{13}$$

Further support to this scaling of the collective Soret coefficient with compressibility comes from a study of polymer blends [66], where, far away from the mixture critical point, S_T is found to be proportional to the zero-wavevector limit $S(0)$ of the static structure factor.

Phase equilibria in colloidal and soft matter systems are the most evident manifestation of collective effects. So far, however, investigations of thermophoresis close to the structural phase transition are very scarce. An interesting exception is study of the glass transition of PS in toluene [67]. While both D and D_T rapidly vanish approaching the glass transition temperature, S_T is totally insensitive to the structural arrest of the system. Since the glass transition is just a kinetic effect, bearing no structural change, this is consistent with the formerly stated relation between S_T and $S(0)$. It is also useful to compare this result with the preliminary observations made by Rusconi *et al* [40] on a nonionic surfactant solution approaching a liquid-crystal phase boundary where, conversely, S_T seems to vanish rather sharply. It is however evident that further studies of simpler phase transition phenomena, such the formation of colloidal crystal in hard-sphere colloidal suspensions, would be extremely useful.

5. Theory

In this section we provide a brief introduction to the methods and assumptions usually introduced for the theoretical interpretation of particle thermophoresis in colloidal suspensions. The included material is not meant to be exhaustive and the adopted perspective mainly reflects our own perception of the subject.

5.1. Brownian motion and the Soret coefficient

An *ab initio* approach to thermophoresis should start with the analysis of the distribution function of a binary mixture in the presence of a thermal gradient [68]. However, when dealing with a suspension of spherical colloidal particles in a solvent we may take advantage of the large difference in the timescales for the dynamics of the two components: the solvent molecules and the colloids. In the limit of extreme dilution, the interactions between colloids can also be neglected, simplifying the problem to the case of a single particle undergoing Brownian motion in a solvent maintained in an external temperature gradient. As previously noted, and discussed in [69], the structure of the temperature profile decouples from the dynamics of the colloid, the timescale for thermal diffusivity being much shorter than that for Brownian motion. Then, the temperature profile quickly equilibrates while the colloid moves. Let us assume that a simple linear dependence $T(z) = T_0 + z\nabla T$ (with ∇T constant) represents the temperature distribution in the cell. In order to evaluate the transport coefficients, the analysis is performed to linear order in ∇T.

Most of the theoretical studies of the Soret effect in dilute colloidal suspensions are based on the Smoluchowski equation describing the time evolution of the probability $P(\mathbf{x}, t)$ to find the colloid at position $\mathbf{x}$:

$$\frac{\partial P}{\partial t} = \nabla\cdot\left[-\frac{P}{f}\mathbf{f} + D\nabla P\right]. \tag{14}$$

Here $\mathbf{f}$ is the external force field acting on the colloid, while f is the friction coefficient, which is usually given by Stokes' law: $f = 6\pi\eta a$ (a is the particle radius and η is the viscosity of

the solvent). Finally, D is the diffusion coefficient, related to f by the Einstein relation $fD = kT$. The stationary solution for a low density suspension of N Brownian particles of mass m then becomes $kT\nabla c = c\mathbf{f}$, with $c(\mathbf{r}) = NmP(\mathbf{r})$. Comparing to the definition of the Soret coefficient (3), we are led to the basic equation

$$S_T \nabla T = -\beta \mathbf{f} \tag{15}$$

where $\beta = 1/k_B T$. Note that in applying the Smoluchowski equation to thermophoretic phenomena, $\mathbf{f}$ represents the net force exerted by the solvent on the colloid due to the presence of a temperature gradient. It is important to stress that $\mathbf{f}$ is not the total force acting on the colloid: the frictional force is not included in $\mathbf{f}$ but appears separately in the Smoluchowski equation (14). In stationary conditions, if the thermal stochastic force, leading to particle diffusion, is neglected, the total force $\mathbf{F}$ acting on the colloid vanishes identically due to the balance between the net force $\mathbf{f}$ and the frictional force $-f\mathbf{v}$. In this case, the asymptotic thermophoretic velocity $\mathbf{v}_T$ attained by the Brownian particle is simply related to $\mathbf{f}$ by the force balance condition:

$$\mathbf{v}_T = \frac{\mathbf{f}}{f}. \tag{16}$$

The main difference among the several approaches proposed so far for explaining the thermophoresis in colloidal suspensions lies in the way the force $\mathbf{f}$ (or equivalently the velocity $\mathbf{v}_T$) is evaluated.

In order to calculate $\mathbf{f}$, we choose to work in the reference frame comoving with the colloid, which is placed at the origin of the coordinate system. The distribution function of the surrounding fluid is modified by the presence of the colloid and of the temperature gradient. In the colloid reference frame, a macroscopic fluid motion sets in: the velocity profile tends to a finite value ($-v_T$ along z) at large distance and momentum is transferred from the fluid to the colloid.

5.2. Linear response theory and hydrodynamics

As a first step, it is convenient to study, within linear response theory, the phase space distribution of a classical fluid in a non-uniform temperature profile. This problem has been investigated in the framework of dilute systems [25] on the basis of a Boltzmann equation approach since the works of Maxwell, Reynolds [22] and Chapman [19]. In the case of strongly interacting systems, like liquids, a convenient starting point is the general formalism by Mori which provides the expressions for the distribution functions to linear order [70].

In the comoving reference frame, the external potential $V(\mathbf{r})$ acting on the solvent due to the presence of the colloid clearly includes a hard core term and, possibly, other contributions. The Hamiltonian of the fluid is given by the standard form:

$$\hat{H} = \sum_i \left[\frac{\mathbf{p}_i^2}{2m} + V(\mathbf{r}_i) \right] + \frac{1}{2} \sum_{i \neq j} v(r_{ij}) \tag{17}$$

where $v(r)$ is the two body interaction between the molecules of the fluid. Here, the phase space functions are denoted by a hat and the dependence on the phase space coordinates $(\mathbf{p}_i, \mathbf{r}_i)$ is understood. At equilibrium, the distribution function is given by $\hat{F}_0 = \frac{1}{Z} e^{-\beta \hat{H}}$ but, when a non-uniform temperature profile $T(\mathbf{x})$ is present or if we allow for a velocity field $\mathbf{v}(\mathbf{x})$ in the fluid, this expression is modified. Following Mori, as a first guess we can introduce the local equilibrium distribution:

$$\hat{F}_{LE} = \frac{1}{Z} \exp\left[-\beta \int d\mathbf{x} \frac{T}{T(\mathbf{x})} \hat{E}(\mathbf{x}) \right] \tag{18}$$

where the phase space function $\hat{E}$ is given by

$$\hat{E}(\mathbf{x}) = \hat{\mathcal{H}}(\mathbf{x}) - \hat{\mathbf{j}}(\mathbf{x}) \cdot \mathbf{w}(\mathbf{x}) \tag{19}$$

in terms of the local energy density $\hat{\mathcal{H}}(\mathbf{x})$ and the momentum density $\hat{\mathbf{j}}(\mathbf{x})$ defined in [70]. The relationship between the auxiliary field $\mathbf{w}(\mathbf{x})$ and the physical fluid velocity $\mathbf{v}(\mathbf{x})$ follows from the identity $\langle \hat{\mathbf{j}}(\mathbf{x}) \rangle = \rho(\mathbf{x})\mathbf{v}(\mathbf{x})$, where $\rho(\mathbf{x})$ is the local mass density of the solvent. An important assumption, at the very basis of the hydrodynamic formalism, is that the fields $T(\mathbf{x})$, $\mathbf{w}(\mathbf{x})$ and $V(\mathbf{x})$ vary slowly in space, i.e. are basically constant on the scale of the correlation length of the fluid. In the case of gases, this assumption corresponds to a vanishing Knudsen number. Outside this regime, it is not possible to adopt Mori's formalism and the concept of local equilibrium cannot be applied. Even when local equilibrium can be defined, the corresponding distribution (18) is not stationary but evolves in time. Following the notation of [70], to linear order in the temperature and velocity field, $\hat{F}(t)$ is given by

$$\hat{F}(t) = \hat{F}_{LTE} + \beta \hat{F}_0 \int d\mathbf{x} \left[\hat{j}^a(\mathbf{x}) w^a(\mathbf{x}) - \int_0^t d\tau \hat{U}(\tau) \left(\hat{J}^{ab}(\mathbf{x}) \partial_b w^a(\mathbf{x}) + \hat{J}_H^a(\mathbf{x}) \frac{\partial_a T(\mathbf{x})}{T} \right) \right] \tag{20}$$

where the local thermal equilibrium (LTE) distribution function $\hat{F}_{LTE}$ does not include the $\mathbf{w}$ term present in (18) and (19), being explicitly taken into account, to first order, in equation (20). Summation over repeated indices is understood. The time evolution operator $\hat{U}(\tau)$ describes the exact dynamics of the many body system with Hamiltonian (17) while the operators $\hat{\rho}(\mathbf{x})$, $\hat{j}^a(\mathbf{x})$, $\hat{J}^{ab}(\mathbf{x})$ and $\hat{J}_H^a(\mathbf{x})$ are respectively the local mass density, mass current, momentum flux tensor and heat flux. The explicit expressions of these operators are available in textbooks [70]. These quantities obey conservation laws: in stationary conditions their divergence equals the contribution induced by the presence of the external potential $V(\mathbf{r})$ in the Hamiltonian (17). This leads to the (linearized) hydrodynamic equations: the continuity equation, the Navier–Stokes (NS) equation and the heat transport equation. When only the hard core contribution is included in $V(\mathbf{r})$, the external potential just reduces to a boundary condition on the hydrodynamic fields, at least on length scales larger than the correlation length of the solvent molecules.

We first evaluate the averages of the previously introduced fluxes by use of the perturbed distribution (20) taking into account the isotropy of the phase space distribution $\hat{F}_0$ (in the absence of an external potential) and working to linear order in the deviations from isotropy. By enforcing the weak spatial dependence of the external fields $\mathbf{w}(\mathbf{x})$ and $T(\mathbf{x})$ on the scale

of the fluid correlation length, the formal expressions of the conserved fluxes become

$$\langle \hat{j}^a(\mathbf{r})\rangle = \beta w^b(\mathbf{r}) \int d\mathbf{x}\langle \hat{j}^a(\mathbf{r})\hat{j}^b(\mathbf{x})\rangle_0 - \beta \frac{\partial_b T(\mathbf{r})}{T} \int d\mathbf{x} \int_0^\infty d\tau \langle \hat{j}^a(\mathbf{r})\hat{U}(\tau)\hat{J}_H^b(\mathbf{x})\rangle_0 \quad (21)$$

$$\langle J^{ab}(\mathbf{r})\rangle = P^{ab}(\mathbf{r}) - \beta\partial_c w^d(\mathbf{r}) \times \int d\mathbf{x} \int_0^\infty d\tau \langle \delta\hat{J}^{ab}(\mathbf{r})\hat{U}(\tau)\delta\hat{J}^{cd}(\mathbf{x})\rangle_0 \quad (22)$$

$$\langle \hat{J}_H^a(\mathbf{r})\rangle = \beta w^b(\mathbf{r}) \int d\mathbf{x}\langle \hat{J}_H^a(\mathbf{r})\hat{j}^b(\mathbf{x})\rangle_0 - \beta \frac{\partial_b T(\mathbf{r})}{T} \int d\mathbf{x} \int_0^\infty d\tau \langle \hat{J}_H^a(\mathbf{r})\hat{U}(\tau)\hat{J}_H^b(\mathbf{x})\rangle_0. \quad (23)$$

The symbol $\langle\cdots\rangle_0$ represents a thermal equilibrium average with distribution function $\hat{F}_0$, $P^{ab}(\mathbf{r}) = \langle \hat{J}^{ab}(\mathbf{r})\rangle_{\mathrm{LTE}}$ is the average of the pressure tensor in local thermal equilibrium while $\delta\hat{J}^{ab}(\mathbf{r}) = \hat{J}^{ab}(\mathbf{r}) - p\delta^{ab}$ is the dissipative part of the pressure tensor. The explicit evaluation of the equilibrium averages gives the expected known results:

$$\int d\mathbf{x}\langle \hat{j}^a(\mathbf{r})\hat{j}^b(\mathbf{x})\rangle_0 = \delta^{ab}kT\rho \quad (24)$$

$$\int d\mathbf{x} \int_0^\infty d\tau \langle \delta\hat{J}^{ab}(\mathbf{r})\hat{U}(\tau)\delta\hat{J}^{cd}(\mathbf{x})\rangle_0 = -kT\left[(\tfrac{2}{3}\eta - \zeta)\delta^{ab}\delta^{cd} - \eta(\delta^{ac}\delta^{bd} + \delta^{ad}\delta^{bc})\right] \quad (25)$$

$$\int d\mathbf{x}\langle \hat{J}_H^a(\mathbf{r})\hat{j}^b(\mathbf{x})\rangle_0 = \delta^{ab}kT(\epsilon + p) \quad (26)$$

$$\int d\mathbf{x} \int_0^\infty d\tau \langle \hat{j}^a(\mathbf{r})\hat{U}(\tau)\hat{J}_H^b(\mathbf{x})\rangle_0 = \rho\Lambda\delta^{ab} \quad (27)$$

$$\int d\mathbf{x} \int_0^\infty d\tau \langle \hat{J}_H^a(\mathbf{r})\hat{U}(\tau)\hat{J}_H^b(\mathbf{x})\rangle_0 = kT^2\kappa\delta^{ab} \quad (28)$$

where η and ζ are the usual shear and bulk viscosity coefficients, κ is the thermal conductivity of the solvent and Λ is an off-diagonal transport coefficient involving cross-correlations between heat and mass flow. ϵ represents the internal energy per unit volume, so that $\epsilon + p$ is the enthalpy density. We stress that these results are exact for homogeneous systems, but this is enough for linear response theory. When equations (24)–(28) are substituted into expressions (21)–(23) we obtain the mass, momentum and energy flux correct to linear order in the external fields. Recalling that, to linear order, $\langle \hat{j}^a(\mathbf{r})\rangle = \rho v^a(\mathbf{r})$, from equation (21) we find the relationship between physical velocity $\mathbf{v}$ and the auxiliary field $\mathbf{w}$:

$$\mathbf{v}(\mathbf{r}) = \mathbf{w}(\mathbf{r}) - \lambda\nabla T \quad (29)$$

where $\lambda = \frac{\Lambda}{kT^2}$. Setting to zero the divergence of the mass, momentum and heat flux, we find the usual stationary conditions for an incompressible fluid:

$$\partial_b w^b = 0 \quad (30)$$

$$\eta\nabla^2 w^a = \partial_b P^{ab} \quad (31)$$

$$\nabla^2 T = 0 \quad (32)$$

which coincide with the linearized hydrodynamic equations in the presence of an anisotropic pressure tensor, with no explicit reference to the existence of a thermal gradient. The temperature profile clearly enters the pressure tensor $P^{ab}(\mathbf{r})$ (evaluated in local thermal equilibrium) but also affects the definition of the auxiliary field $\mathbf{w}(\mathbf{r})$ entering the NS equation, which does not coincide with the physical mass velocity $\mathbf{v}(\mathbf{r})$ as shown by equation (29). This circumstance seems to support the approach put forward by Brenner [71, 72] but, by substituting $\mathbf{w} = \mathbf{v} + \lambda\nabla T$ into equations (30)–(32), we find that the same equations hold for the physical velocity field $\mathbf{v}(\mathbf{r})$, showing that the mixing implied by equation (29) is ineffective and does not provide the microscopic interpretation of thermophoretic phenomena. However, the off-diagonal contribution Λ plays an important role in defining the momentum distribution of the solvent in a thermal gradient. When the distribution (20) is specialized to the case of a homogeneous, static gas ($\mathbf{v} = 0$, $\rho \to 0$) in a thermal gradient, we recover a well known result of the kinetic theory of gases: in the low density limit, the single-particle momentum distribution function of a fluid particle is indeed affected by a thermal gradient according to equation (5) and deviates from the equilibrium value [20], while the pressure tensor remains uniform throughout the fluid.

The microscopic approach briefly reviewed here shows that thermophoretic phenomena, both in gases and in liquids, can be interpreted on the basis of the usual hydrodynamic equations (30)–(32) in the presence of either an explicit colloid–solvent interaction or of interfacial effects which trigger anisotropies in the pressure tensor P^{ab} close to the colloid [33, 69].

5.3. *Interfacial effects and the problem of boundary conditions*

We now discuss the explicit solution of equations (30) and (31) including the consequences of an anisotropic pressure tensor in the NS equation but neglecting the detailed structure of the temperature profile close to the colloid.

In the colloid reference frame, we have just to solve the linearized NS equation

$$\eta\nabla^2 v^a = \partial_b P^{ab} \quad (33)$$

for an incompressible fluid (i.e. with $\mathrm{div}\mathbf{v} = 0$). As already shown in equation (22), $P^{ab}(\mathbf{r})$ is evaluated in local thermal equilibrium. In the absence of a temperature gradient, the spherical symmetry of the problem forces the pressure tensor to depend only on two scalar functions [74]:

$$P^{ab} = p_{\mathrm{T}}(r)\delta^{ab} + \left[p_{\mathrm{N}}(r) - p_{\mathrm{T}}(r)\right]n^a n^b. \quad (34)$$

In LTE, the temperature dependence of the pressure tensor is converted into spatial dependence by setting $T \to T(z)$:

$$p_{\mathrm{N}} \to p_{\mathrm{N}}(r) + \nabla T\frac{\partial p_{\mathrm{N}}}{\partial T}z \qquad p_{\mathrm{T}} \to p_{\mathrm{T}}(r) + \nabla T\frac{\partial p_{\mathrm{T}}}{\partial T}z. \quad (35)$$

The formal structure of the NS equation (33) with such a pressure tensor coincides with the expression already studied in [75], whose solution can be obtained analytically. A

solenoidal velocity field in cylindrical symmetry may be parametrized in terms of a single scalar function $\phi(r)$ as [73]

$$\mathbf{v} = \mathbf{n}z\frac{\mathrm{d}}{\mathrm{d}r}\left(\frac{\phi'}{r}\right) - \mathbf{k}\left(v_{\mathrm{T}} + \frac{\phi'}{r} + \phi''\right) \tag{36}$$

where a prime represents derivation with respect to the radial coordinate and $(\mathbf{n}, \mathbf{k})$ are the unit vectors in the radial and z directions respectively. By substituting this parametric form into equation (33) we find the explicit expression for $\phi'(r)$:

$$\phi'(r) = \frac{1}{2\eta}I_2(r) - \frac{r}{3\eta}I_1(r) - \frac{1}{6\eta r^2}I_4(r) - \frac{B}{r^2} + A \tag{37}$$

where, as usual, A and B are integration constants which can be obtained by imposing the appropriate boundary conditions. The integrals $I_n(r)$ are given by

$$I_n(r) = \int_r^\infty \mathrm{d}r r^n \psi(r) \tag{38}$$

where the function ψ, assumed to be short range, is written in terms of the normal component of the anisotropic part of the pressure tensor:

$$\psi = -\frac{1}{2}\nabla T\frac{\partial}{\partial T}\left[rp'_{\mathrm{N}} + 3p_{\mathrm{N}}\right]. \tag{39}$$

This solution also requires that the components $(p_{\mathrm{N}}, p_{\mathrm{T}})$ of the unperturbed pressure tensor satisfy the hydrostatic equilibrium condition. Finally, it is useful to provide the explicit expression of the normal component of the total stress tensor

$$n^b(P^{ab} + \sigma^{ab}) = n^a\Bigg[p_{\mathrm{N}} + z\frac{\partial p_{\mathrm{N}}}{\partial T}\nabla T - \eta z\left(\frac{\phi'''}{r} - 4\frac{\phi''}{r^2} + 4\frac{\phi'}{r^3}\right)\Bigg] + \eta k^a\phi'''. \tag{40}$$

Integrating this form on a spherical surface of radius r we obtain the net momentum flux. By substituting the solution $\phi'(r)$ (37) several simplifications occur and we simply get

$$\text{Outgoing momentum flux} = -8\pi\eta A\mathbf{k} \tag{41}$$

showing that, as implied by momentum conservation, the momentum flux through every spherical surface is constant, independently from the chosen boundary condition. The total force acting on the colloid is then simply given by

$$F_z = 8\pi\eta A. \tag{42}$$

The force balance condition $\mathbf{F} = 0$ then gives $A = 0$, which, together with the chosen boundary condition at the colloid surface, defines the asymptotic velocity v_{T} and the Soret coefficient S_{T}, via equations (15) and (16).

The inner boundary condition has to be chosen according to the specific features of the solvent–colloid interface. Without entering these details, we may investigate three commonly adopted boundary conditions, respectively named stick (or no-slip), slip, and Navier.

5.3.1. Stick boundary conditions. In this case we impose that on the colloid surface the fluid velocity field vanishes: $\mathbf{v}(\mathbf{r})|_a = 0$. By use of equations (36) and (37) the two integration constants A and B are easily obtained. The vanishing of the total force leads, via equation (42), to $A = 0$ and then to

$$\mathbf{v}_{\mathrm{T}} = \frac{2}{3\eta a}\left[aI_1(a) - I_2(a)\right]\mathbf{k} = -\frac{\nabla T}{3\eta}\frac{\partial}{\partial T} \times \int_a^\infty \mathrm{d}r(r-a)\left(1 + \frac{a}{r}\right)\left[p_{\mathrm{N}} - p_{\mathrm{T}}\right] \tag{43}$$

which, via equations (15) and (16), gives the Soret coefficient for stick boundary conditions:

$$S_{\mathrm{T}} = 2\pi\beta a\frac{\partial}{\partial T}\int_a^\infty \mathrm{d}r(r-a)(1 + \frac{a}{r})(p_{\mathrm{N}} - p_{\mathrm{T}}). \tag{44}$$

This equation relates the Soret coefficient to the temperature derivatives of the components of the pressure tensor. Expression (44) closely resembles the definition of the surface tension γ for a spherical surface:

$$\gamma = \int_a^\infty \mathrm{d}r\frac{a}{r}(p_{\mathrm{N}} - p_{\mathrm{T}}) \tag{45}$$

and shows that the Soret coefficient is basically proportional to the temperature derivative of the product between the surface tension and the width ℓ of the fluid layer characterized by an anisotropic pressure tensor (the so called transition layer):

$$\ell\gamma = \int_a^\infty \mathrm{d}r(r-a)(p_{\mathrm{N}} - p_{\mathrm{T}}). \tag{46}$$

Such a result conforms to the common structure of the phoretic coefficients proposed by Ruckenstein [33] and implies a linear dependence of the Soret coefficient on the particle radius. As discussed in section 4.2.3, this dependence is experimentally verified for microemulsion droplets in a non-polar solvent, although it is still not universally accepted for colloidal latex particles (see figure 2). Regarding the temperature dependence, we note that a deeper investigation of the colloid–solvent interface is required for a quantitative comparison between theory and experiments. However, as shown in [76], in a dense fluid, both the surface tension γ and the characteristic length ℓ depend on temperature only through the number density of the fluid, leading to a general result: the Soret coefficient is proportional to the thermal expansion of the solvent, at least when the colloid–solvent interactions are confined to their interface.

5.3.2. Slip boundary conditions. Alternatively, we may impose slip boundary conditions at the colloid surface: the normal component of the velocity field must clearly vanish, while the other condition is given by the vanishing of the tangential component of the surface stress,

$$0 = t^a(P^{ab} + \sigma^{ab})n^b = \eta t^a k^a\phi'''(a) \tag{47}$$

which implies the vanishing of $\phi'''(a)$. Here the tangential unit vector is defined as $\mathbf{t} = \partial\mathbf{n}/\partial\theta$. By inserting the explicit form (37) we again determine the two integration constants A

and B. The thermophoretic velocity and the Soret coefficient then follow from equations (15) and (16):

$$S_T = \frac{4}{3}\pi\beta a \frac{\partial}{\partial T}\int_a^\infty dr\, r\,(p_N - p_T). \tag{48}$$

This result is very different from what has been obtained in the case of stick boundary conditions, showing that the accurate treatment of surface effects plays a key role in thermophoretic phenomena. The Soret coefficient is again basically proportional to the temperature derivative of the surface tension (45) times a characteristic length that now coincides with the particle radius a rather than the width of the transition layer as before. Expression (48) closely resembles that obtained by Würger [77], who neglected the anisotropy of the pressure tensor (and the presence of external forces acting on the fluid due to the colloid) but imposed a phenomenological inner boundary condition expressing the balance between the surface stress and the 'Marangoni force':

$$\eta t^a n^b(\partial_a v^b + \partial_b v^a) + t^a \partial_a \gamma(T(z)) = 0. \tag{49}$$

The only difference between equation (48) and Würger's expression of S_T is in the dependence on thermal conductivity, which is absent in our approach due to the chosen form of the temperature gradient. Note that the scaling of the two estimates (44) and (48) on the colloid radius a is different, being now quadratic, rather than linear as in equation (44). The dependence of S_T on the chosen boundary conditions has also been recently remarked in [78].

5.3.3. Navier boundary conditions. Following Ajdari [31], we now investigate the so called 'Navier' boundary condition. Besides the vanishing of the normal component of the velocity at the colloid surface, we now allow the tangential velocity $\mathbf{t}\cdot\mathbf{v} = v_t$ to remain finite at $r = a$. Let us define b as the distance from the surface (inside the colloid) where the linearly extrapolated v_t vanishes:

$$b\left.\frac{\partial v_t}{\partial r}\right|_{r=a} = v_t|_{r=a}. \tag{50}$$

The calculations are carried out following the usual steps and lead to a more general formula for the Soret coefficient. Remarkably, the result can be written as the linear combination of the two expressions (44) and (48) in the suggestive form

$$S_T = 4\pi a\beta \frac{a-b}{a+2b}\frac{\partial}{\partial T}\left\{\ell\gamma\left[1 + \frac{a}{a-b}\frac{b}{\ell}\right]\right\}. \tag{51}$$

Following the argument put forward by Ajdari, we now specialize to the case of $\ell \ll b \ll a$. This corresponds to small deviations from stick boundary conditions and a small width of the fluid layer influenced by the presence of the colloid. In this case, $a/(a-b) \simeq 1$ and the expression in parenthesis just reproduces the enhancement factor introduced in [31].

5.4. Failure of the energy route

We now briefly compare the above results, based on detailed hydrodynamic calculations, with the class of approaches aiming at the evaluation of the net force on the colloid $\mathbf{f}$ in terms of temperature derivatives of a suitably defined free energy. The starting point of this group of theories is the possibility to write the net force $\mathbf{f}$ as the gradient of a potential:

$$\mathbf{f} = -\nabla U. \tag{52}$$

In a one dimensional geometry this equation does not impose any restriction on the form of the force. The point is that the potential $U(T(z))$ is usually identified as a thermodynamic quantity: the internal energy of the colloidal suspension [79–81], the Gibbs free energy [44] or the 'reversible work' [82]. In all cases, the energy $U(T)$ can be written as a volume term plus a surface contribution:

$$U(T) = \Delta\epsilon\tfrac{4}{3}\pi a^3 + \gamma 4\pi a^2 \tag{53}$$

where $\Delta\epsilon$ is the difference between a free energy density of the colloid and that of the fluid while γ is the surface tension of the colloid–solvent interface. Inserting (53) into equation (52) we get

$$\mathbf{f} = -\nabla U = -\left.\frac{dU}{dT}\right|_p \nabla T = -\left[\frac{d\Delta\epsilon}{dT}\frac{4}{3}\pi a^3 + \frac{d\gamma}{dT}4\pi a^2\right]\nabla T. \tag{54}$$

The first term is considered in [81], where the temperature derivative of the internal energy is identified as a specific heat. Other papers ignore the volume term and concentrate on the surface tension contribution, which has been evaluated in the specific case of charged colloids.

In order to comment on the validity of these approaches we have to ask whether the net force acting on the colloid may be indeed expressed as the derivative of some (free/internal) energy of the system. A first objection rests upon the fact that minimum principles hold only at thermodynamic equilibrium, while thermophoresis refers to stationary states. Even circumventing this difficulty, a purely thermodynamic approach may just give information on the total force acting on the colloid. However, as already noted in section 5.1, the total force on the colloid vanishes identically in a stationary state: the Soret coefficient just depends on the net force, which equals the opposite of the frictional force. Therefore it is not possible to identify the net force if hydrodynamic effects are neglected.

5.5. Remarks on electrostatic effects

The physically relevant case of charged colloids poses additional problems related to the dynamics of the counterions present in solution. Several papers address this problem, but the results strongly depend on the assumed structure of the screening cloud, and in particular on the drag of the solvent on the charge carriers. Sometimes a further Smoluchowski equation is written for both co-and counterions [83]. Other authors [78] assume a local thermal equilibrium distribution of charges, thereby adopting the equilibrium Boltzmann distribution. Alternatively, a continuity equation for the counterion motion is written [69]. Most importantly, when the theoretical analysis is employed for the interpretation of experiments, other physical phenomena should be considered,

like the dependence of the charge on the colloid and of the surface potential on the salinity of the solution or the charge renormalization due to short range interactions at the surface [84].

6. Conclusions and perspectives

From all we have said, thermophoresis turns out to be a very challenging effect, requiring novel experimental and theoretical efforts to be fully understood. Beside its interest for basic statistical mechanics as one of the simplest non-equilibrium effects, it is also very promising for practical applications to particle manipulation.

New investigation techniques, and in particular particle-tracking schemes, can surely be devised. Since there is actually no need for *resolving* single particles through high numerical-aperture optics, but simply detecting the position of their center of mass, methods such as ultramicroscopy, where the particle position is detected just by imaging against a dark background the diffraction-limited spot of the light scattered off-axis, could work reasonably well. Fourier-space methods, with their distinctive property of performing an intrinsic average over the motion of many particles, can also be very promising. While usual methods such as homodyne intensity correlation spectroscopy (dynamic light scattering) probe only relative particle motion, new scattering methods such as space–time resolved correlation (STRC) or near field scattering (NFS) are conversely very sensitive to *absolute* particle drift. In STRC [85], a 'speckled' image of the sample is formed by using a stopped-down lens system with small entrance pupil. The intensity of each single speckle fluctuates on a timescale set by D and by the observation angle, while collective particle drift yields a uniform translation of the speckle field (so that the effects of particle Brownian motion and of thermophoretic drift are easily discriminated). NFS consists in measuring spatial correlations in the scattering speckle field close to the sample, which, at variance with the far field speckle pattern, bears direct information on particle spatial correlation. Since NFS experiments are more conveniently made at small scattering angle in a *homodyne* configuration [86], where the scattered and transmitted intensities are made to interfere, they are again sensitive to absolute particle motion. Scattering concepts and techniques, moreover, being familiar to colloid scientists, may attract a larger community towards studies of thermophoretic effects. There is also ample room to extend our present knowledge of thermophoretic effects by performing more extensive investigations of surfactant, polyelectrolyte, and biomacromolecular solutions or by directly visualizing the thermophoretic motion for big particles.

As concerns the present status of the theory, the analysis we have developed in section 5 has hopefully established some reference points, namely the following. (i) The presence of a thermal gradient alone in a dense liquid does not induce a thermophoretic force. (ii) A direct microscopic interaction between colloid and solvent is required to give rise to particle thermophoresis. (iii) If the effects of such an interaction may be represented in terms of a non-trivial structure of the pressure tensor at the interface, the Soret coefficient can be written in the form (51). (iv) The boundary conditions at the colloid–solvent interface strongly affect the scaling of S_T with the particle radius, which turns out to be linear only in the case of stick boundary conditions. (v) On general grounds, the Soret coefficient for 'athermal' colloids is expected to be proportional to the thermal expansivity of the solvent.

The rapid growth of microfluidics techniques opens up a number of possible application of thermophoresis, both for practical and basic reasons. Indeed, while exploiting dielectrophoretic effects, the most common method used to manipulate colloidal particles, is feasible and efficient for insulating suspensions, conductive aqueous systems require applying high-frequency electric fields to avoid electrode polarization, and measurements often suffer by noticeable Joule heating, while thermophoresis is obviously totally immune from these spurious effects. Moreover, while dielectrophoresis or electrophoresis rely on simple particle properties such as dielectric constant or surface charge, thermophoresis allow taking advantage of multifarious aspects of particle/solvent interactions. For instance, we have seen that different proteins, even with a similar charge value, may display an opposite sign of S_T, so that a mixture could in principle be fractionated by thermophoretic methods. Furthermore, most experiments seem to show, and theory to support, that D_T is insensitive to particle size. A size-independent mobility makes thermophoretic transport a better strategy, compared to motion induced for example dielectrophoresis or magnetophoresis, where the mobility scales with the square of the particle radius, to study small colloids. The application of a steady temperature difference ΔT leads to a steady-state fractional concentration difference at the sides of a microfluidic channel of width d given by $\Delta c/c = S_T \Delta T$, which is reached in a timescale $\tau \simeq d^2/\pi^2 d$. Assuming for instance $d = 50\ \mu$m, $\Delta T = 10\,^\circ$C, we get $\Delta c/c \simeq 22.5\%$, $\tau \simeq 5$ s for NaPSS with $M_w = 74$ kDa, which is not a small effect. Thermophoretic separation in microfluidic devices has been recently obtained by Geelhoed *et al* [87]. Although preliminary, these results are rather promising for downsizing microfluidics into the nanometric world.

References

[1] Poon W C K 2004 *Science* **304** 830
[2] Buzzaccaro S, Rusconi R and Piazza R 2007 *Phys. Rev. Lett.* **99** 098301
[3] Tyrrell J V 1961 *Diffusion and Heat Flow in Liquids* (London: Buttherworths)
[4] Ludwig C 1859 *Sitz. Ber. Akad. Wiss. Wien* **20** 539
[5] Soret C 1879 *Arch. Sci. Phys. Nat.* **2** 48
[6] de Groot S R 1945 *L'Effet Soret, Diffusion Thermique Dans Les Phasescondensées* (Amsterdam: North-Holland)
[7] La Porta A and Surko C M 1998 *Phys. Rev. Lett.* **80** 3759
[8] Zheng L L, Larson D J and Zheng H 1998 *J. Cryst. Growth* **191** 243
[9] Cygan R T and Carrigan C R 1992 *Chem. Geol.* **95** 201
[10] Busser F H 1989 *Mantle Convection: Plate Tectonics and Global Dynamics* ed W R Peltier (New York: Gordon and Breach)
[11] Cross M C and Honenberg P C 1993 *Rev. Mod. Phys.* **65** 851
[12] Vailati A and Giglio M 1998 *Phys. Rev.* E **58** 4361
[13] Chapman S 1912 *Phil. Trans. R. Soc.* A **211** 433

[14] Wiegand S 2004 *J. Phys.: Condens. Matter* **16** R357
[15] Artola P-A and Rousseau B 2007 *Phys. Rev. Lett.* **98** 125901
[16] Giglio M and Vendramini A 1975 *Phys. Rev. Lett.* **34** 561
[17] Mistura L 1972 *Nuovo Cimento* B **12** 35
[18] Tyndall J 1870 *Proc. R. Inst. G. B.* **6** 1
[19] Chapman S 1928 *Proc. R. Soc.* A **119** 34
[20] Maxwell J C 1879 *Phil. Trans. R. Soc.* **170** 231
[21] Brush S G 1976 *The kind of Motion We Call Heat* (Amsterdam: Elsevier)
[22] Kennard E H 1938 *Kinetic Theory of Gases* (New York: McGraw-Hill) chapter 8
[23] Epstein P S 1929 *Z. Physik* **54** 537
[24] Rosner D E 1980 *Physicochem. Hydrodyn.* **1** 159
[25] Zheng F 2002 *Adv. Colloid Interface Sci.* **97** 255
[26] Sone Y 2002 *Kinetic Theory and Fluid Dynamics* (Boston: Birkhäuser) chapter 3
[27] Dobbins R A and Megaridis C M 1987 *Langmuir* **3** 254
[28] de la Mora J and Mercer J M 1982 *Phys. Rev.* A **26** 2178
[29] Derjaguin B V, Churaev N V and Muller V M 1987 *Surface Forces* (New York: Consultants Bureau)
[30] Anderson J L 1989 *Ann. Rev. Fluid Mech.* **21** 61
[31] Ajdari A and Bocquet L 2006 *Phys. Rev. Lett.* **96** 186102
[32] Derjaguin B V and Sidorenkov G P 1941 *Dokl. Acad. Nauk SSSR* **32** 622
[33] Ruckenstein E 1981 *J. Colloid Interface Sci.* **83** 77
[34] Ecenarro O, Madariaga J A, Navarro J, Santamaria C M, Carrion J A and Saviron J M 1990 *J. Phys.: Condens. Matter* **2** 2289
[35] Jones R C and Furry F H 1946 *Rev. Mod. Phys.* **18** 151
[36] Putnam S A and Cahill D G 2005 *Langmuir* **21** 5317
[37] Gordon J P, Leite R C C, Moore R S, Porto S P S and Whinnery J R 1965 *J. Appl. Phys.* **36** 3
[38] Bialkowski S E 1996 *Photothermal Spectroscopy Methods for Chemical Analysis* (New York: Wiley)
[39] Giglio M and Vendramini A 1974 *Appl. Phys. Lett.* **25** 555
[40] Rusconi R, Isa L and Piazza R 2004 *J. Opt. Soc. Am.* B **21** 605
[41] Köhler W and Schäfer R 2000 *New Developments in Polymer Analytics* II (Berlin: Springer)
[42] Hartung M and Köhler W 2007 *Rev. Sci. Instrum.* **78** 084901,
[43] Duhr S, Arduini S and Braun D 2004 *Eur. Phys. J.* E **15** 277
[44] Duhr S and Braun D 2006 *Phys. Rev. Lett.* **96** 168301
[45] Braibanti M, Vigolo D and Piazza R 2008 *Phys. Rev. Lett.* **100** 108303
[46] Ning H, Buitenhuis J, Dhont J K G and Wiegand S 2006 *J. Chem. Phys.* **125** 204911
[47] Blums E, Odenbach S, Mezulis A and Maiorov M 1998 *Phys. Fluids* **10** 2155
[48] Piazza R and Guarino A 2002 *Phys. Rev. Lett.* **88** 208302
[49] Iacopini S, Rusconi R and Piazza R 2006 *Eur. Phys. J.* E **19** 59
[50] Ning H, Kita R, Kriegs H, Luettmer-Strathmann J and Wiegand S 2006 *J. Chem. Phys.* **110** 10746
[51] Vigolo D, Brambilla G and Piazza R 2007 *Phys. Rev.* E **75** 040401(R)
[52] Iacopini S and Piazza R 2003 *Europhys. Lett.* **63** 247
[53] Braun D and Libchaber A 2002 *Phys. Rev. Lett.* **89** 188103
[54] Brochard F and De Gennes P-G 1981 *C. R. Acad. Sci., Paris* II **293** 1025
[55] Schimpf M E 2000 *Thermal Nonequilibrium Phenomena in Fluid Mixtures* ed S Wiegand and W Köhler (Berlin: Springer)
[56] Rauch J and Köhler W 2003 *J. Chem. Phys.* **119** 11977
[57] Zhang K J, Briggs M E, Gammon R W, Sengers J V and Douglas J F 1999 *J. Chem. Phys.* **111** 2270
[58] Rauch J and Köhler W 2004 *Macromolecules* **38** 3571
[59] Rauch J, Hartung M, Privalov A F and Köhler W 2007 *J. Chem. Phys.* **126** 214901
[60] Kita R and Wiegand S 2005 *Macromolecules* **38** 4554
[61] Kita R, Kircher G and Wiegand S 2004 *J. Chem. Phys.* **121** 9140
[62] Sugaya R, Wolf B A and Kita R 2006 *Biomacromolecules* **7** 435
[63] Putnam S A, Cahill D G and Wong G C L 2007 *Langmuir* **23** 9221
[64] Kita R, Wiegand S and Luettmer-Strathmann J 2004 *J. Chem. Phys.* **121** 3874
[65] Happel J and Brenner H 1965 *Low Reynolds Number Hydrodynamics* (Englewood Cliffs, NJ: Prentice-Hall)
[66] Enge W and Köhler W 2004 *Phys. Chem. Chem. Phys.* **6** 2373
[67] Rauch J and Köhler W 2002 *Phys. Rev. Lett.* **88** 185901
[68] Goldhirsch I and Ronis D 1983 *Phys. Rev.* A **27** 1616
[69] Morozov K I 1999 *JETP* **88** 944
[70] Balescu R 1975 *Equilibrium and Nonequilibrium Statistical Mechanics* (New York: Wiley) chapter 21
[71] Brenner H 2005 *Physica* A **349** 60
[72] Bielenberg J and Brenner H 2005 *Physica* A **356** 279
[73] Landau L D and Lifshitz E M 1959 *Fluid Mechanics* (New York: Pergamon)
[74] Schofield P and Henderson J R 1982 *Proc. R. Soc. Lond.* A **379** 231
[75] Parola A and Piazza R 2004 *Eur. Phys. J.* E **15** 255
[76] Parola A and Piazza R 2005 *J. Phys.: Condens. Matter* **17** S3639
[77] Würger A 2007 *Phys. Rev. Lett.* **98** 138301
[78] Fayolle S, Bickel T and Würger A 2007 *Preprint* 0709.0384
[79] Bringuier E and Bourdon A 2003 *Phys. Rev.* E **67** 011404
[80] Fayolle S, Bickel T, Le Boiteux S and Würger A 2005 *Phys. Rev. Lett.* **95** 208301
[81] Würger A 2006 *Europhys. Lett.* **74** 658
[82] Dhont J K G, Wiegand S, Duhr S and Braun D 2007 *Langmuir* **23** 1674
[83] Rasuli S N and Golestanian R 2007 *Preprint* 0708.0090
[84] Belloni L 1985 *J. Chem. Phys.* **99** 43
[85] Cipelletti L, Bissig H, Trappe V, Ballesta P and Mazoyer S 2003 *J. Phys.: Condens. Matter* **15** S257
[86] Brogioli D, Vailati A and Giglio M 2002 *Appl. Phys. Lett.* **81** 4109
[87] Geelhoed P F, Lindken R and Westerweel J 2006 *Chem. Eng. Res. Des.* **84** 370